Contributions of the 8-Methyl Group to the Vibrational Normal Modes of Flavin Mononucleotide and Its 5-Methyl Semiquinone Radical

Azaria S. Eisenberg and Johannes P. M. Schelvis*

Department of Chemistry, New York University, 100 Washington Square East, New York, New York 10003

Received: December 17, 2007; Revised Manuscript Received: March 31, 2008

Resonance Raman spectroscopy is a powerful tool to investigate flavins and flavoproteins, and a good understanding of the flavin vibrational normal modes is essential for the interpretation of the Raman spectra. Isotopic labeling is the most effective tool for the assignment of vibrational normal modes, but such studies have been limited to labeling of rings II and III of the flavin isoalloxazine ring. In this paper, we report the resonance and pre-resonance Raman spectra of flavin mononucleotide (FMN) and its N5-methyl neutral radical semiquinone (5-CH_3FMN$^{\bullet}$), of which the 8-methyl group of ring I has been deuterated. The experiments indicate that the Raman bands in the low-frequency region are the most sensitive to 8-methyl deuteration. Density functional theory (DFT) calculations have been performed on lumiflavin to predict the isotope shifts, which are used to assign the calculated normal modes to the Raman bands of FMN. A first assignment of the low-frequency Raman bands on the basis of isotope shifts is proposed. Partial deuteration of the 8-methyl group reveals that the changes in the Raman spectra do not always occur gradually. These observations are reproduced by the DFT calculations, which provide detailed insight into the underlying modifications of the normal modes that are responsible for the changes in the Raman spectra. Two types of isotopic shift patterns are observed: either the frequency of the normal mode but not its composition changes or the composition of the normal mode changes, which then appears at a new frequency. The DFT calculations also reveal that the effect of H/D-exchange in the 8-methyl group on the composition of the vibrational normal modes is affected by the position of the exchanged hydrogen, i.e., whether it is in or out of the isoalloxazine plane.

Flavoproteins are ubiquitous in nature and perform many physiologically important reactions.[1,2] They are capable of both oxidizing and reducing various substrates and play an important role in electron transfer.[2–4] The flavin cofactor can accept or donate one or two electrons at a time, and this unique ability enables it to function as an intermediary between two-electron donors and one-electron acceptors.[2–4] The most common flavin molecules found in flavoproteins are riboflavin (RF), flavin mononucleotide (FMN), and flavin adenine dinucleotide (FAD). Flavins can exist in three different oxidation states: oxidized, radical semiquinone, and fully reduced hydroquinone. Under physiological conditions, the semiquinone and hydroquinone can be anionic ($pK_a = 8.5$) or neutral ($pK_a = 6.7$), respectively.[1,2] The flavin semiquinone is not stable in solution due to the disproportionation of two semiquinones to one oxidized and one reduced flavin.[2,5] Semiquinones can be stabilized in proteins and micelles[6–8] and by chemical modification.[9,10]

Many different methodologies are available to study flavins and flavoproteins,[2] and Raman spectroscopy has proven to be an important spectroscopic tool.[11,12] The Raman bands of flavins are sensitive to redox and protonation state of the isoalloxazine ring, hydrogen bonding interactions involving the isoalloxazine ring, steric interactions, solvent polarity, and planarity of the isoalloxazine ring.[11–15] A good understanding of their vibrational normal modes is essential for the interpretation of Raman spectra of flavin molecules. Isotopic labeling of riboflavin has been used to interpret the Raman spectra of oxidized riboflavin and its anionic radical semiquinone.[16,17] These data in combination with computational approaches, ranging from normal coordinate to density functional theory (DFT) calculations, have been used for the normal mode assignment of oxidized flavins.[18–25] Normal mode assignments have also been proposed for the anionic and neutral hydroquinone forms of FAD,[26] but only a few isotope spectra are available for the flavin neutral radical semiquinone, for which a partial normal mode assignment was recently proposed on the basis of H/D- exchange experiments and DFT calculations.[27–32]

Raman spectroscopy of isotopically labeled flavins has been limited to substitutions in rings II and III of the isoalloxazine ring (Figure 1). Although isotopic labeling of ring I is possible, multiple carbon atoms are labeled with various degrees of enrichment,[33] which makes the interpretation of isotope shifts in vibrational spectra difficult. Flavins have been chemically modified by replacement of the 7- and 8-methyl groups of ring I to obtain more insight in ring I vibrational modes.[27,34–38] These chemical modifications can affect the electronic structure of the isoalloxazine ring, potentially changing its structure from benzenoid to quinonoid.[37,38] Such changes in the electron density throughout the isoalloxazine ring complicate the analysis of the Raman spectra because of potential changes in bond orders, normal coordinate composition, and Raman excitation profiles, which in turn affect peak positions and intensities throughout the spectra. Its use in the assignment of flavin Raman bands is therefore limited.

It is desirable to make a simple isotopic substitution at ring I, and especially, at the 8-position because the 8-methyl group may have a functional role in several proteins and enzymes. For example, monoamine oxidase has a covalent thioether bond

* Corresponding author. Current address: Department of Chemistry and Biochemistry, Montclair State University, 1 Normal Av., Montclair, NJ 07043. Tel: 973-655-3301. Fax: 973-655-7772. E-mail: schelvisj@mail.montclair.edu.

10.1021/jp711832g CCC: $40.75
Published on Web 06/12/2008

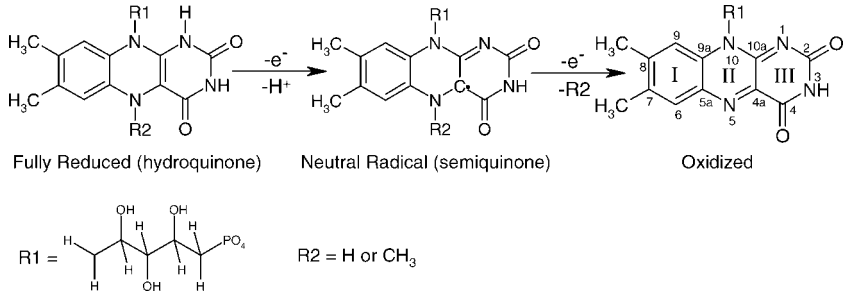

Figure 1. Structures and atomic numbering of the isoalloxazine ring for the oxidation of the 1,5-dihydroquinone to the neutral radical semiquinone and the oxidized FMN.

between the protein matrix and FAD at the 8-position.[39,40] The 8-methyl group is also of potential interest in electron-transfer processes in reductase domains and in photolyases. In NADPH P450 reductase, the 8-methyl carbon of FAD is about 4 Å away from the 8- and 7-methyl carbons of FMN,[41] which may provide an important electron tunneling pathway. In DNA photolyase, the cyclobutane pyrimidine dimer (CPD) has one carbonyl oxygen that is only 4.3 Å away from the 8-methyl carbon of the FAD cofactor, which may provide a direct electron-transfer pathway from the FAD to the CPD lesion in the DNA-repair mechanism.[42] Resonance Raman experiments showed that substrate binding perturbs hydrogen-bonding interactions between FAD and the protein matrix, which also changes the $FADH^-/FADH^\bullet$ reduction potential.[31,43] On the basis of a very small shift in a ring I mode, it has been proposed that the CPD may interact with the 8-methyl group of FAD.[44] However, the contribution of the 8-methyl group to this normal mode or to any flavin normal mode has never been established.

In this work, we are particularly interested in identifying vibrational normal modes that are associated with the 8-methyl group of the isoalloxazine ring. We have deuterated the 8-methyl group of FMN, and we have collected the resonance and preresonance Raman spectra of oxidized FMN and resonance Raman spectra of the neutral radical semiquinone of 5-methyl FMN. We have also performed DFT calculations and compared calculated isotope shifts to the experimentally observed ones. This combined experimental and computational approach has facilitated the assignment of vibrational normal modes to Raman bands that are sensitive to the 8-methyl group and provided insight into their behavior upon 8-methyl deuteration. Finally, analysis of spectra where the 8-methyl group was partially deuterated provides new insight into how stepwise 8-methyl deuteration changes the flavin normal modes.

Materials and Methods

Materials. D_2O was purchased from Cambridge Isotope Laboratories. All other chemicals were purchased from Sigma-Aldrich and used without further purification.

Synthesis of 8-Methyl Deuterated FMN (8MD-FMN). Deuteration of the 8-methyl group of FMN was done following a literature procedure.[45] FMN (0.24 g) was dissolved in 10 mL of D_2O (0.2 M phosphate, pD = 6.7), making a 0.05 M solution, which was refluxed at 95 °C. Samples were collected at regular intervals to monitor the progress of the deuteration reaction by ^1H NMR spectroscopy (Bruker, Avance-400). Complete deuteration of the 8-methyl group was accomplished after refluxing the solution for 5 h and was confirmed by capillary LC/MSD TrapXCT (Agilent 1100 Series) and ^1H NMR spectroscopy. The product was purified by isocratic reversed-phase HPLC (JASCO PU-987) with a C18 column (microsorb MV, Varian) using 0.005 M tetrabutylammonium phosphate as the mobile phase at 1 mL/min.[46] Because freshly synthesized and HPLC-purified 8MD-FMN were indistinguishable in our experiments, we omitted the purification step.

Synthesis of the 5-Methyl FMN Neutral Radical. The 5-methyl FMN neutral radical ($5\text{-}CH_3FMN^\bullet$) was made following literature procedures with small modifications.[9,10] Sodium cyanoborohydrate (0.14 g) was dissolved in 1 mL of 2.2 M formaldehyde in water, making a 2.2 M solution. The solution was deoxygenated by using three cycles each of 5 min of vacuum followed by 5 min of flushing with N_2. Concurrently, FMN (5 mg) and sodium dithionite (56 mg) were added to 2 mL of water containing 0.5 M sodium acetate (potassium phosphate in the case of 8-MD FMN) to buffer the solution at pH 4.5. This solution was also deoxygenated following the procedure described above. The sodium dithionite immediately reduced FMN to $FMNH_2$, and the $FMNH_2$ solution was transferred with a gastight syringe to the sodium cyanoborohydrate solution in 4 mL glass vials sealed with rubber septa, which were used as reaction vessels. This solution was stirred for 1 h, after which the synthesis of fully reduced $5\text{-}CH_3FMN$ was completed. $5\text{-}CH_3FMN^\bullet$ was prepared by removing 10−100 μL from the stock solution and adding it to 60−700 μL aerated water, upon which the fully reduced $5\text{-}CH_3FMN$ was oxidized to $5\text{-}CH_3FMN^\bullet$. The formation and concentration of $5\text{-}CH_3FMN^\bullet$ were confirmed by UV−vis spectroscopy.

Electronic Absorption and Raman Spectroscopy. Electronic absorption spectra were recorded with a UV−vis spectrophotometer (Lambda 40, Perkin-Elmer). For the resonance Raman spectra, the samples were diluted to 10^{-4}−10^{-5} M in deionized and distilled water or D_2O, which included 1 M KI to quench fluorescence. The samples were placed in a spinning Raman cell and sealed with a rubber septum to avoid unwanted air oxidation of $5\text{-}CH_3FMN^\bullet$. The resonance Raman spectra were collected with the system described elsewhere.[31] The samples were excited with the 406.7 nm (FMN) and 530.9 nm ($5\text{-}CH_3FMN^\bullet$) lines from a Kr^+ laser (I-302, Coherent). The preresonance Raman spectra of FMN were obtained with the 647.1 nm line of the Kr^+ laser. The Raman scattered light was collimated by a lens (f = 50 mm), and Rayleigh scattering was removed by using a 647 nm holographic notch filter (Kaiser Optical). The Raman scattered light was focused (f = 200 mm) into a Triax 320 spectrometer (JY/Horiba) and was dispersed with a 1200 mm^{-1} groove grating and detected with a N_2(l)-cooled, front-illuminated, open-electrode CCD detector (Symphony, JY/Horiba). The Raman spectra were calibrated with the known spectrum of toluene, and Origin 7.0 (OriginLab) was used for data analysis.

Calculations. The geometries of lumiflavin and the neutral radical of $5\text{-}CH_3$ lumiflavin were optimized by using density functional theory (DFT) calculations with the B3LYP functional[47] and the 6-31G(d,p) basis set[48] in Spartan '02 (Wave

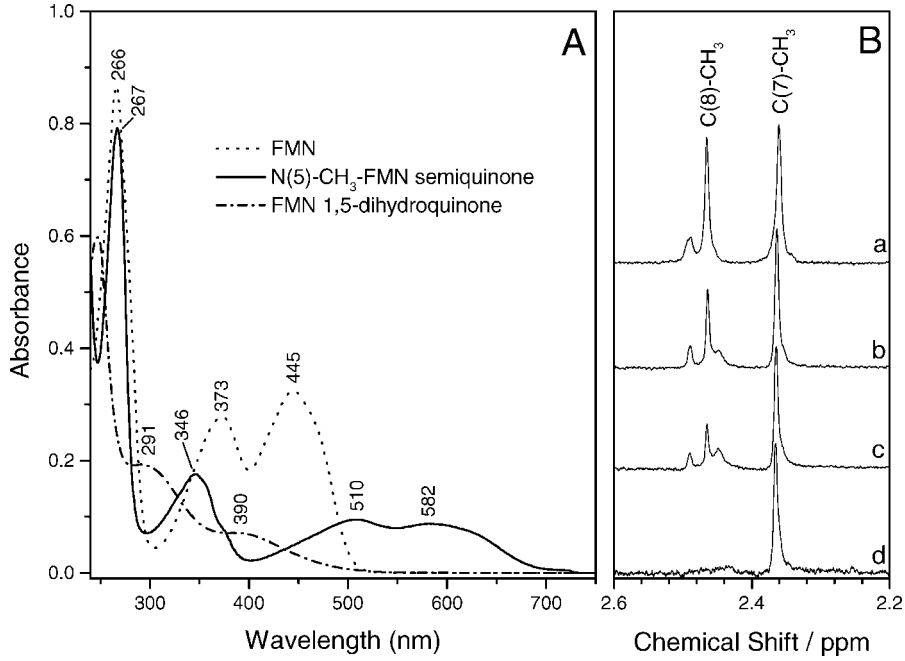

Figure 2. (A) Absorption spectra of $FMNH_2$ (—), 5-$CH_3FMN^{\bullet}$ (—•—), and FMN (•••) in H_2O. (B) ^1H NMR spectra showing the gradual deuteration of the 8-methyl group of FMN by the disappearance of its ^1H-resonance at 2.47 ppm after 0 (a), 20 (b), 45 (c), and 300 min (d) of the H/D-exchange reaction.

function) on a QS12−2000R cluster (Parallel Quantum Solutions).[49] The optimized geometry was used as input for Gaussian 98 on an Origin200 (Silicon Graphics) of the Academic Computer Services at New York University.[50] The DFT method with the B3LYP functional and 6-31G(d,p) basis set were used for geometry reoptimization and for calculation of the vibrational normal modes, their frequencies and Raman intensities. DFT calculations overestimate the harmonic frequencies and various scaling methods have been proposed to correct for this.[51–54] The scaled quantum mechanics force field method gives the best results but requires a set of scaling parameters for each specific class of molecules.[51–53,55–57] Such scaling parameters are currently not available for flavin molecules. Furthermore, we will assign the vibrational normal modes by comparing observed and predicted isotope shifts, which depend more on the normal mode composition than on the scaling of the harmonic frequencies. Therefore, we decided to use a global scaling factor of 0.9614 to correct the calculated frequencies.[54] Visualization of the optimized molecules and of their vibrational modes was done by using the gOpenMol package.[58]

Results

Characterization of 5-$CH_3FMN^{\bullet}$ and 8-CD_3-FMN. Figure 1 shows the atomic numbering and structures of flavin mononucleotide (FMN) and 5-$CH_3FMN^{\bullet}$ that are important for the experiments in this study, which were conducted at pH 4.5. The absorption spectra of FMN, its 1,5-dihydroquinone ($FMNH_2$), and its 5-methyl neutral radical semiquinone (5-$CH_3FMN^{\bullet}$) are shown in Figure 2A. FMN and $FMNH_2$ have absorption maxima at 445, 373, and 266 nm and at 390, 291, and 248 nm, respectively. The neutral radical semiquinone flavin is the only flavin redox form that absorbs above 510 nm,[2] and 5-$CH_3FMN^{\bullet}$ has absorption maxima at 267, 346, 510, and 582 nm, which is in excellent agreement with literature values.[10]

Figure 2B shows the methyl region of the ^1H NMR spectrum of FMN at 0, 20, 45, and 300 min following the C8−CH_3/D_3 exchange reaction. The protons of the 7- and the 8-methyl groups have resonances at 2.4 and 2.5 ppm, respectively.[45] As the H/D-exchange reaction proceeds, the 2.5 ppm peak diminishes due to progressive deuteration of C8−CH_3 and has completely disappeared after 5 h, at which time the reaction was stopped. The successful C8−CH_3/D_3 exchange was verified by the increase in mass by 3 amu for 8MD-FMN compared to FMN (data not shown).

Resonance Raman Spectra of FMN and 8MD-FMN. Figure 3 shows the high- and low-frequency resonance Raman spectra of FMN and 8MD-FMN in H_2O and in D_2O, which results in N3−H/D exchange. For conformity, the standard labeling of the flavin Raman bands is used.[18,37] In the high-frequency region, 8-methyl deuteration does not affect bands I, III, VII, and X at 1630, 1551, 1355, and 1260 cm^{-1}, respectively. Bands II, IV, V, and IX at 1583, 1502, 1464, and 1281 cm^{-1} have small frequency downshifts upon 8-methyl deuteration with two minor bands at 1453 and 1440 cm^{-1} disappearing. In contrast, bands VI, XI, XII, and XIII at 1410, 1228, 1184, and 1160 cm^{-1} and the bands at 1145 and 1065 cm^{-1} show a frequency upshift for 8-MD FMN, of which the 8 cm^{-1} increase in frequency of band XI is the most noticeable change. In D_2O, the bands above 1350 cm^{-1} are not affected by N3−H/D exchange and show the same response to 8-methyl deuteration as in H_2O solution. However, N3−H/D exchange dramatically affects the Raman bands between 1050 and 1350 cm^{-1}, which has been assigned to uncoupling of δ(ND) from these normal modes upon N3−H/D exchange.[59–61] For the labeling of the Raman bands of FMN in D_2O, we have used the suggested assignments for riboflavin.[60]

In the low-frequency region, several Raman bands show significant frequency shifts upon 8-methyl deuteration of FMN. The 834 cm^{-1} band seems to shift by −29 cm^{-1} to 805 cm^{-1}, and bands at 611 and 505 cm^{-1} shift by −9 cm^{-1} to 602 and 496 cm^{-1}, respectively. The intense, narrow band at 742 cm^{-1} appears to split into two new ones at 729 and 738 cm^{-1}, and the bands at 788, 682, 539, and 426 cm^{-1} show a small decrease in frequency upon 8-methyl deuteration. All bands except those

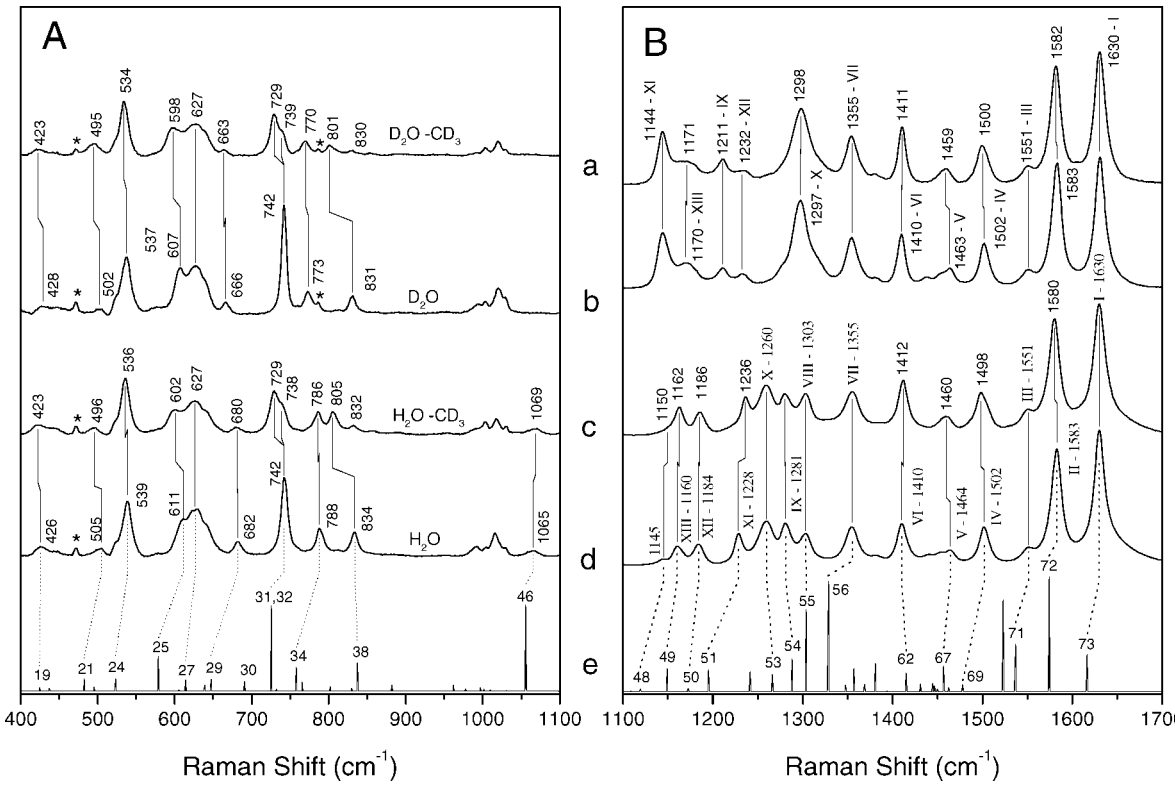

Figure 3. High- and low-frequency resonance Raman spectra of 8MD-FMN (a) and FMN in D_2O (b) and of 8MD-FMN (c) and FMN in H_2O (d). All spectra were taken in the presence of 1 M KI and with excitation at 406.7 nm. Calculated Raman spectrum of lumiflavin with scaled frequencies (e). The dotted lines indicate the assignments of the calculated normal modes to the observed Raman bands.

at 742 and 627 cm^{-1} are sensitive to the N3−H/D exchange in D_2O. In D_2O, the same behavior is observed for 8-methyl deuteration as in H_2O, indicating that the N3−H/D and C8−CH_3/D_3 exchanges do not dramatically change the normal modes that are associated with these Raman bands. In most cases, the effect of the C8−CD_3 and N3−D isotopes on the Raman frequencies is additive as can be seen in Table 1.

Pre-resonance Raman Spectra of FMN and 8MD-FMN. The 8-methyl deuteration gives rise to the same frequency shifts in the (pre-resonance) Raman spectra of FMN (Figure 4). However, a small band appears at 1445 cm^{-1} in the Raman spectrum of 8MD-FMN, while the two minor bands at 1453 and 1440 cm^{-1} of FMN actually disappear in the resonance Raman spectrum upon 8-methyl deuteration. Band XI shows the same 8 cm^{-1} upshift upon complete 8-methyl deuteration, but a weak band remains at 1227 cm^{-1}. Band X is not very intense in the Raman spectrum of FMN in D_2O, and a minor band at 1274 cm^{-1}, similar to the 1276 cm^{-1} band of RF in riboflavin binding protein (RBP),[14,18] is observed in the D_2O spectrum and shifts to 1260 cm^{-1} upon 8-methyl deuteration. Because no Raman band in H_2O has such a large sensitivity to 8-methyl deuteration, the origin of the 1274 cm^{-1} band cannot be identified at this point. Finally, one of the carbonyl stretching modes (νC═O) is observed at 1709 cm^{-1}, which has a slight sensitivity (−2 cm^{-1}) to 8-methyl deuteration and a known sensitivity (−10 cm^{-1}) to N3−H/D exchange.[14,62]

Gradual Deuteration of the 8-Methyl Group. Figure 5 shows the effect of gradual deuteration of the 8-methyl group on the resonance Raman spectrum of FMN in the 1100−1250 cm^{-1} (B) and 550−875 cm^{-1} (A) regions. Spectra are shown for 0%, ∼33%, ∼66%, and 100% 8-methyl deuteration, as determined by NMR spectroscopy. Band XI at 1228 cm^{-1} loses intensity and broadens at the low-frequency side around 1217 cm^{-1} upon partial deuteration. After complete deuteration, the band sharpens and abruptly shifts to 1236 cm^{-1}. In contrast, bands XII and XIII and the one at 1145 cm^{-1} do not visibly broaden upon partial deuteration, but they do abruptly shift after complete deuteration of the 8-methyl group.

Some changes in the low-frequency region are more gradual with progression of the deuteration reaction: the disappearance and appearance of the 834 and 805 cm^{-1} bands, respectively, the decrease in intensity of the 742 cm^{-1} peak combined with the appearance of the 729 cm^{-1} band, and the appearance of the 602 cm^{-1}shoulder. The frequency shift and intensity change of the 682 and 788 cm^{-1} bands occur abruptly and only upon complete deuteration.

Ab Initio Calculations of Lumiflavin. The Raman spectra of lumiflavin (LF) and its C8−D_3 and/or N3−D isotopomers were calculated, and the absence of imaginary frequencies confirmed the proper optimization of their geometries. The coordinates of the optimized geometries and the scaled frequencies are provided in the Supporting Information. The calculated Raman spectrum of LF is shown at the bottom of Figures 3 and 4.

The C8−methyl hydrogens are equivalent in solution because of free rotation about the C8−CH_3 bond. In the calculations, the location and motions of one in-plane (ip) and two out-of-plane (oop) hydrogens can be identified. Therefore, calculation for partial deuteration of C8−CH_3 were done with deuterium atoms in the different positions with respect to the isoalloxazine plane. For single deuteration, we used two models, one with the deuterium in-plane (D_{ip}) and two hydrogens out-of-plane (H_{oop}), and the other one with deuterium out-of-plane (D_{oop}), one hydrogen out-of-plane (H_{oop}) and one in-plane (H_{ip}). For double deuteration, we performed calculations for LF with one model containing ($2D_{oop}$, H_{ip}) and the other one containing (D_{ip}, D_{oop}, H_{oop}).

TABLE 1: Experimental and Calculated Frequencies (cm^{-1}) of FMN[a]

band	observed frequency	no.	calculated frequency	description[c]
	1709 (−2, −9, −12)	75	1745 (0, −1, −1)	$\nu C_4{=}O$, $\nu C_2{=}O$, δNH
	n.o.[b]	74	1735 (0, −11, −11)	$\nu C_2{=}O$, δNH, $\nu C_4{=}O$
I	1630 (0, 0, 0)	73	1617 (−1, 0, −1)	$\nu CC(I)$, $\delta C_{9a}N_{10}C_{10a}$, $\nu C_{4a}{-}N_5$
II	1583 (−3, 0, −1)	72	1574 (−1, 0, −1)	$\nu C_{4a}{-}N_5$, $\nu C_{10a}{-}N_1$, $\nu C_8{-}C_9$, $\nu C_{9a}{-}N_{10}$
III	1551 (0, 0, 0)	71	1537 (−1, 0, −2)	$\nu_a N_1{-}C{-}{-}N_{10}$, $\nu C_{9a}{-}{-}C_{5a}$, $\nu_a C_8{-}C_7{-}C_6$
IV	1501 (−3, 0, −1)	69	1478 (−2, 0, −2)	$\nu_a C_m{-}C_8{-}C_7$, $\nu_a C_m{-}C_7{-}C_8$, $\nu CC(I)$, δCH
V	1464 (−4, −1, −5)	67	1457 (−3, 0, −3)	methyl def, νCN (II), $\nu CC(I)$
VI	1410 (+2, 0, +1)	62	1415 (+6, 0, +6)	methyl def, νCN (II), $\nu CC(I)$
VII	1355 (0, 0, 0)	56	1328 (0, −1, −1)	νCC(I, II, III), δNH, νCN(II, III)
VIII	1303 (0, −, −)	55	1304 (0, 0, 0)	rings(II, III, I), δNH, δC_6H
IX	1281 (−1, −71, −71)	54	1288 (−2, 0, −2)	rings(II, I, III), $\delta N_{10}{-}C{-}H_{oop}$, δC_8CH_{ip}
X	1260 (0, +37, +38)	53	1266 (0, +3, +3)	rings(I, II), δCH, $\nu N_{10}{-}C_m$, δNH, $\nu C_7{-}C_m$
XI	1228 (+8, −84, −84)	51	1195 (+8, −10, −1)	rings(I, III), δCH, $\nu C_8{-}C_m$, $\nu C_7{-}C_m$, δNH
XII	1184 (+2, +48, +48)	50	1174 (+2, −, −)	rings(III, II, I), δC_6H, $\nu C_8{-}C_m$, δNH
XIII	1160 (+2, +10, +11)	49	1149 (+2, +12, +12)	rings(II, III), δCH, δNH, $\nu C_8{-}C_m$
	1145 (+5, −, −)	48	1119 (+14, +1, +14)	$\nu C_8{-}C_m$, $\nu C_7{-}C_m$, δC_6H, $\nu N_{10}{-}C_m$, ring(I)
	1065 (+4, −, −)	46	1056 (+12, −7, +4)	rings(I, II), $\nu C_7{-}C_m$, $\nu C_8{-}C_m$, δNH
	834 (−29, −3, −33)	38	837 (−16, −4, −20)	rings(III, II), δCH, $\nu C_8{-}C_m$, $\delta C_mC_7C_6$
		36	802 (−26, −3, −29)	rings(II, III, I), $\delta C_9C_8CH_{ip}$
	788 (−2, −15, −18)	34	758 (−7, −22, −27)	rings(I, II, III), $\nu C_7{-}C_m$, δNH, $\delta C_{10a}N_{10}C$
	742 (−4, 0, −3)	31	725 (−1, −2, −3)	twists, $\delta_{oop}CH$, $\delta_{oop}NH$
	742 (−13, 0, −13)	32	725 (−13, 0, −13)	ring(I), $\nu C_8{-}C_m$, $\delta C_6C_7C_m$
		30	690 (−1, −32, −37)	δ_{oop}(NH), twists
	682 (−2, −16, −18)	29	647 (−4, −23, −25)	ring(II), δNH, δCO, $\nu C_8{-}C_m$
	627 (0, 0, 0)	27	614 (−2, −1, −3)	rings(I, II), $\delta C_6C_7C_m$, $\delta C_{9a}N_{10}C_m$
	611 (−9, −4, −13)	25	579 (−10, −4, −14)	rings(III, II), $\delta C_8C_7C_m$, $\delta C_7C_8C_m$
	539 (−3, −2, −5)	24	523 (−8, 0, −8)	ring(II), $\delta C_9C_8C_m$, $\delta C_6C_7C_m$
	505 (−9, −3, −10)	21	482 (−12, −2, −14)	rings(I, III), $\delta C_7C_8C_m$, $\delta C_8C_7C_m$
	426 (−3, +2, −3)	19	424 (−3, −2, −5)	ring(III), $\delta C_6C_7C_m$, $\delta C_9C_8C_m$, δC_2O
		18	387 (−5, −1, −6)	rings(III, I), $\delta C_6C_7C_m$, $\delta C_9C_8C_m$, δC_4O

[a] The observed and calculated shifts (cm^{-1}) are given between parentheses for C8−D_3, N3−D, and C8−D_3/N3−D, respectively. [b] n.o., not observed; [c] Abbreviations: ν, stretch; ν_a, asymmetric stretch; δ, bend; I, ring I: II, ring II; III, ring III; ring(s), combination of stretching and bending of indicated ring(s); def, C−H stretching and/or bending within the methyl groups; ip, in-plane; oop, out-of-plane; δCH, bending of ring I hydrogens; twists, oop twisting motions of atoms in isoalloxazine skeleton.

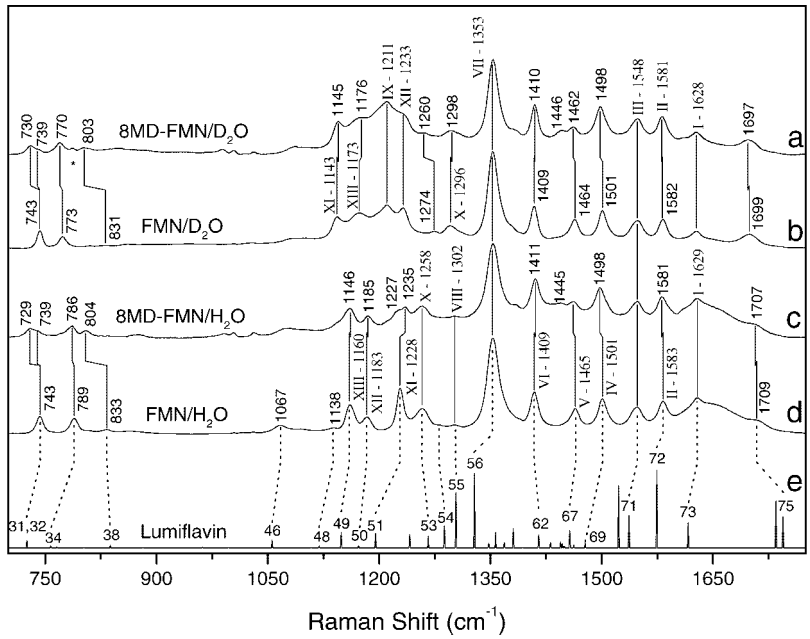

Figure 4. Pre-resonance Raman spectra of 8MD-FMN (a) and FMN (b) in D_2O, and 8MD-FMN (c) and FMN in H_2O (d). All spectra were taken in the presence of 1 M KI and with excitation at 647.1 nm. Calculated Raman spectrum of lumiflavin with scaled frequencies (e). The dotted lines indicate the assignments of the calculated normal modes to the observed Raman bands.

Figure 5 shows the results for two spectral regions of interest, 550−850 cm^{-1} (C) and 1100−1250 cm^{-1} (D), which contain the Raman bands that are most sensitive to 8-methyl deuteration. For partial deuteration, the spectra for C8−CH_2D and for C8−CHD_2 are shown. Although it is likely that partial deuteration results in a mixture of no, single, double, and triple deuteration, the spectra for C8−CH_2D and for C8−CHD_2 are in excellent qualitative agreement with the experimental data. The behavior of the calculated normal modes at 1195, 1174, 1149, and 1119 cm^{-1} (Figure 5D) correlates very well with that

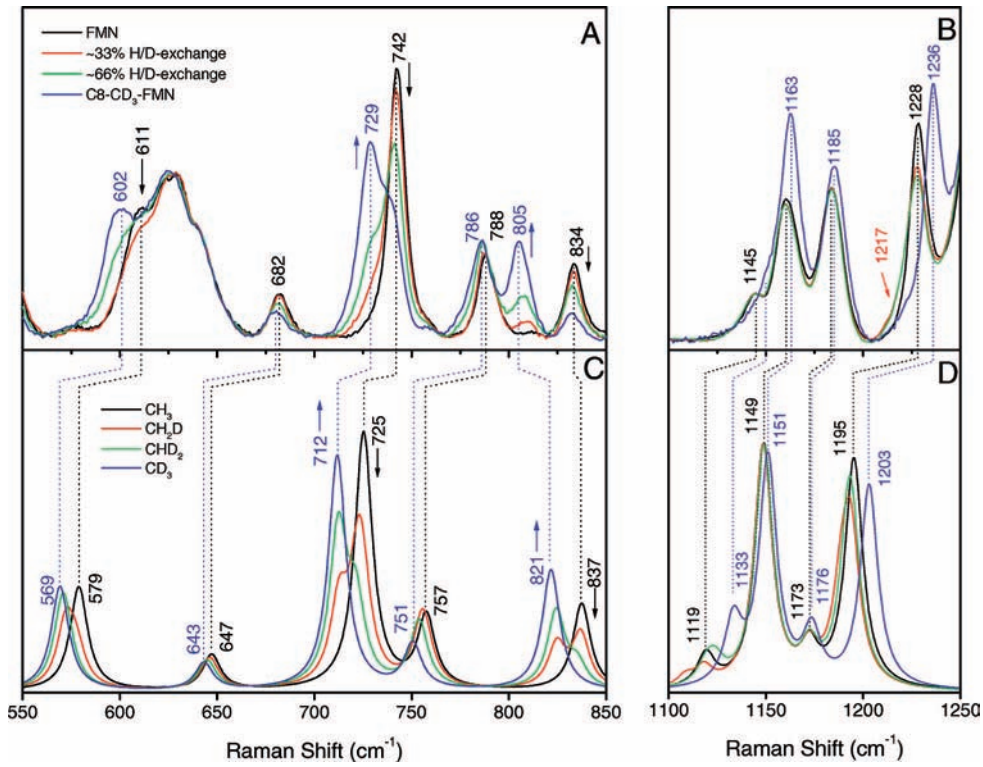

Figure 5. High- (A) and low-frequency (B) resonance Raman spectra of FMN with C8−CH_3 (black), with ∼33% (red) and ∼66% (green) of C8−CH_3 deuteration complete, and C8−CD_3 FMN (blue). All spectra were taken in the presence of 1 M KI and with excitation at 406.7 nm. Calculated Raman spectra of partial deuteration of the 8-methyl group of LF; CH_3 (black), CDH_2 (33% deuterium in-plane, and 66% deuterium out-of-plane), CD_2H (33% both deuteriums out-of-plane, and 66% one deuterium in-plane and one deuterium out-of-plane), and CD_3 (bottom). For clarity, only the normal modes assigned to the Raman bands are shown, and the black and blue dashed lines indicate the normal modes assigned to Raman bands of FMN and 8MD-FMN, respectively. The Raman bands were simulated with a Lorentzian line shape with an 11 cm^{-1} width, which is the average width of the observed Raman bands.

of the observed Raman bands at 1228, 1184, 1160, and 1145 cm^{-1} (Figure 5B), and that of the modes at 837, 757, 725, 647, and 579 cm^{-1} (Figure 5C) shows strong correlation to the bands at 834, 788, 742, 682, and 611 cm^{-1} (Figure 5A). The fact that the calculated and observed gradual deuteration frequency patterns match very well validates our calculations and assignments.

Resonance Raman Spectra of 5-CH_3FMN•. The high-frequency RR spectrum of 5-CH_3FMN• in H_2O (Figure 6B) is characterized by the strong 1612 cm^{-1} band and is similar to the one that was reported before and to those of flavin neutral radical semiquinones (FlH•).[10,28,31,63] Upon C8−CH_3 deuteration, the bands between 1612 and 1480 cm^{-1} shift to a slightly lower frequencies. Three bands around 1431 cm^{-1} seem to condense into one at 1435 cm^{-1}, and the bands between 1380 and 1130 cm^{-1}, except for the 1283 cm^{-1} band, shift to higher frequencies. In D_2O, N3−H/D exchange occurs, and no significant changes occur for Raman bands above 1250 cm^{-1}; the 1450 and 1410 cm^{-1} bands shift down by 3 cm^{-1}, and the 1376, 1335, and 1322 cm^{-1} bands shift up by 2−3 cm^{-1}. The changes of the Raman bands between 1050 and 1250 cm^{-1} are complex; the 1228, 1213, and 1177 cm^{-1} bands converge into a broader band with two distinguishable peaks at 1219 and 1187 cm^{-1}, and the 1131 cm^{-1} band seems to shift to 1108 cm^{-1}.

The low-frequency region of the RR spectrum of 5-CH_3FMN• shows larger changes upon C8−CH_3 deuteration (Figure 6A). The 900−1000 cm^{-1} region is omitted due to contributions from the buffer and the lack of significant 5-CH_3FMN• Raman bands. The bands at 891 and 877 cm^{-1} disappear upon 8-methyl deuteration, probably because of a significant change in their normal modes. The bands at 787, 742, 686, 658, 607, 553, and 531 cm^{-1} shift 3−8 cm^{-1} toward lower frequencies, while the 653, 600, and 524 cm^{-1} bands broaden upon 8-methyl deuteration. When the solvent is changed from H_2O to D_2O, the 891 cm^{-1} band loses intensity and the 877 cm^{-1} band appears to shift to 850 cm^{-1}. The 787 cm^{-1} band changes shape with its peak shifting to 778 cm^{-1}, while the 686 cm^{-1} band shifts to 691 cm^{-1}. The 658 cm^{-1} band seems to split into two bands at 658 and 649 cm^{-1}. The changes in the RR spectrum upon C8−methyl deuteration in D_2O largely mimic those observed in H_2O; the 778 cm^{-1} band, e.g., shifts to a lower frequency just like its equivalent in H_2O. However, the split bands of 5-CH_3FMN• in D_2O at 658 and 649 cm^{-1} seem to condense into a single band at 645 cm^{-1} upon 8-methyl deuteration.

Discussion

Assignment of C8−CH_3 Sensitive Normal Modes of FMN. The 87 normal modes of lumiflavin are numbered 1 through 87 in going from the lowest to the highest frequency. The match between the observed FMN Raman bands and the calculated normal modes of lumiflavin are listed in Table 1 and shown in Figures 3 and 4. Each match is strictly based on the agreement between experimentally observed and theoretically predicted isotope shift patterns. The calculated isotope shifts were determined primarily by visual inspection of all the calculated vibrational modes and, in some cases, by comparing the Raman intensities only between calculated spectra. We allowed only a 34 cm^{-1} difference (average error in calculated frequency after scaling)[54] between observed and calculated frequencies. This restriction had to be relaxed for the 1709 and 682 cm^{-1} Raman bands. For the 1709 cm^{-1} band, isotopic labeling experiments

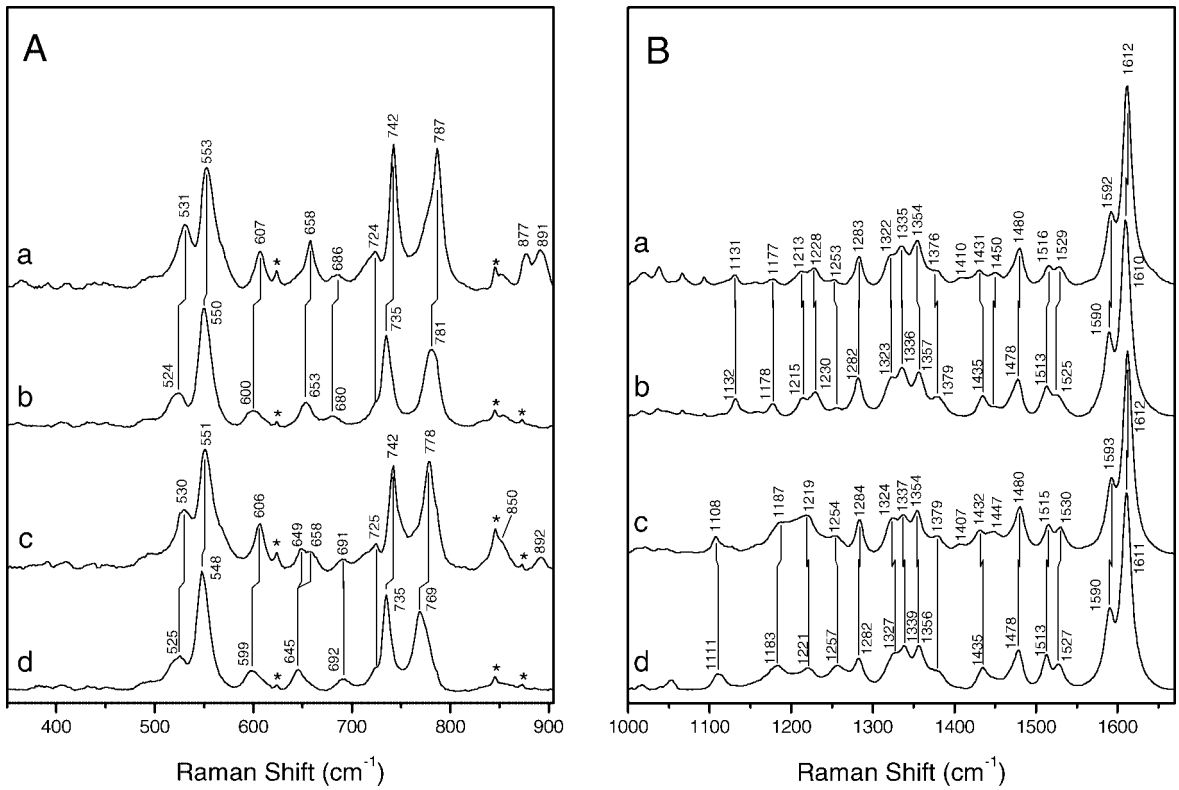

Figure 6. High- and low-frequency resonance Raman spectra of the 5-CH_3FMN$^{\bullet}$ in H_2O (a) and in D_2O (c), and of 8-MD, 5-CH_3FMN$^{\bullet}$ in H_2O (b) and D_2O (d). All spectra were taken in the presence of 1 M KI and with excitation at 530.9 nm.

and investigation of hydrogen-bonding effects provide strong evidence for its assignment to the νC_4═O of mode 75 rather than to the νC_2═O of mode 74.[25,61] For bands VIII−XII, we only used the observed and predicted C8−CD_3 isotope shift for the assignments, because the accompanying normal modes following N3−H/D exchange could not be identified. The N3−H/D isotope shift assignments were taken from the literature.[60] Careful analysis of the calculated normal modes either shows that N3−H/D exchange causes a significant change in their composition, which has been proposed before,[59,60,64] or the suggested N3−H/D band shifts are not all correctly assigned. The latter view is supported by our experiments that show that the proposed band XI in D_2O at 1145 cm^{-1} lacks the 8 cm^{-1} frequency upshift that is observed in H_2O upon C8−CH_3 deuteration. This means that either the normal mode of band XI changes significantly when the solvent is D_2O such that C8−CH_3 deuteration no longer causes any frequency change or the assignment of band XI of flavin in D_2O has to be reconsidered. Although N3−H/D exchanges cause significant scrambling of some normal modes, it should be noted that we did not observe any significant scrambling of the normal modes of the observed Raman bands due to C8−CH_3 deuteration. The root-mean-square of the difference between the observed Raman bands and the calculated normal modes following our assignments is 18.5 cm^{-1}. As expected, the intensities of the calculated Raman spectrum do not compare well to the resonance Raman spectrum, and they are a better match with those of the preresonance Raman spectrum.

In the high-frequency region, the calculated frequencies and normal modes are in very good agreement with earlier DFT calculations.[22−25] We found only one disagreement. Unno et al. assigned band V to a normal mode with mainly deformation of the methyl groups.[25] Our calculations predict that ring I and II stretches also contribute significantly to this normal mode, as much as they do to the one at 1394 cm^{-1} and to band VI, in agreement with others.[22,23] Figure 7 includes vector diagrams of the four normal modes that are most sensitive to C8−CH_3/D_3 exchange in the high-frequency region.

In the low-frequency region, the N3−H/D exchange does not complicate the normal mode assignments much, and the C8−CH_3 deuteration data facilitate most of the assignments. For three of the observed Raman bands, the observed isotope shifts were each predicted equally well by two normal mode candidates (Table 1). For the Raman bands at 834 and 426 cm^{-1}, we favor normal modes 38 and 19, respectively, because their calculated frequencies are closest to the observed ones. For the Raman band at 682 cm^{-1}, we prefer normal mode 29 over 30, because the latter is an out-of-plane mode, which is not expected to have any significant Raman intensity given the planar isoalloxazine ring of FMN.

For the Raman bands of flavin below 1000 cm^{-1}, only assignments based on normal coordinate and semiempirical quantum mechanical calculations are available for comparison.[18−21] The descriptions of the normal modes below 1000 cm^{-1} are quite complicated. In most cases, two or three rings undergo a complex combination of bending and stretching vibrations complemented with bending motions of C═O, NH, CH, and C−CH_3, as well as C−CH_3 stretching and CH_3 rocking motions. The vector diagrams of the six normal modes that are most sensitive to C8−CH_3 are included in Figure 7, and a general description of the normal modes of all observed Raman bands is given in Table 1. We did not find much overlap between our assignments and those made previously,[18−21] because the normal coordinate and semiempirical calculations do not properly take into account the extensive coupling throughout the molecule asserted by the ab initio calculations. However, the assignment of the 742 cm^{-1} band to ring I and the contribution of δC═O

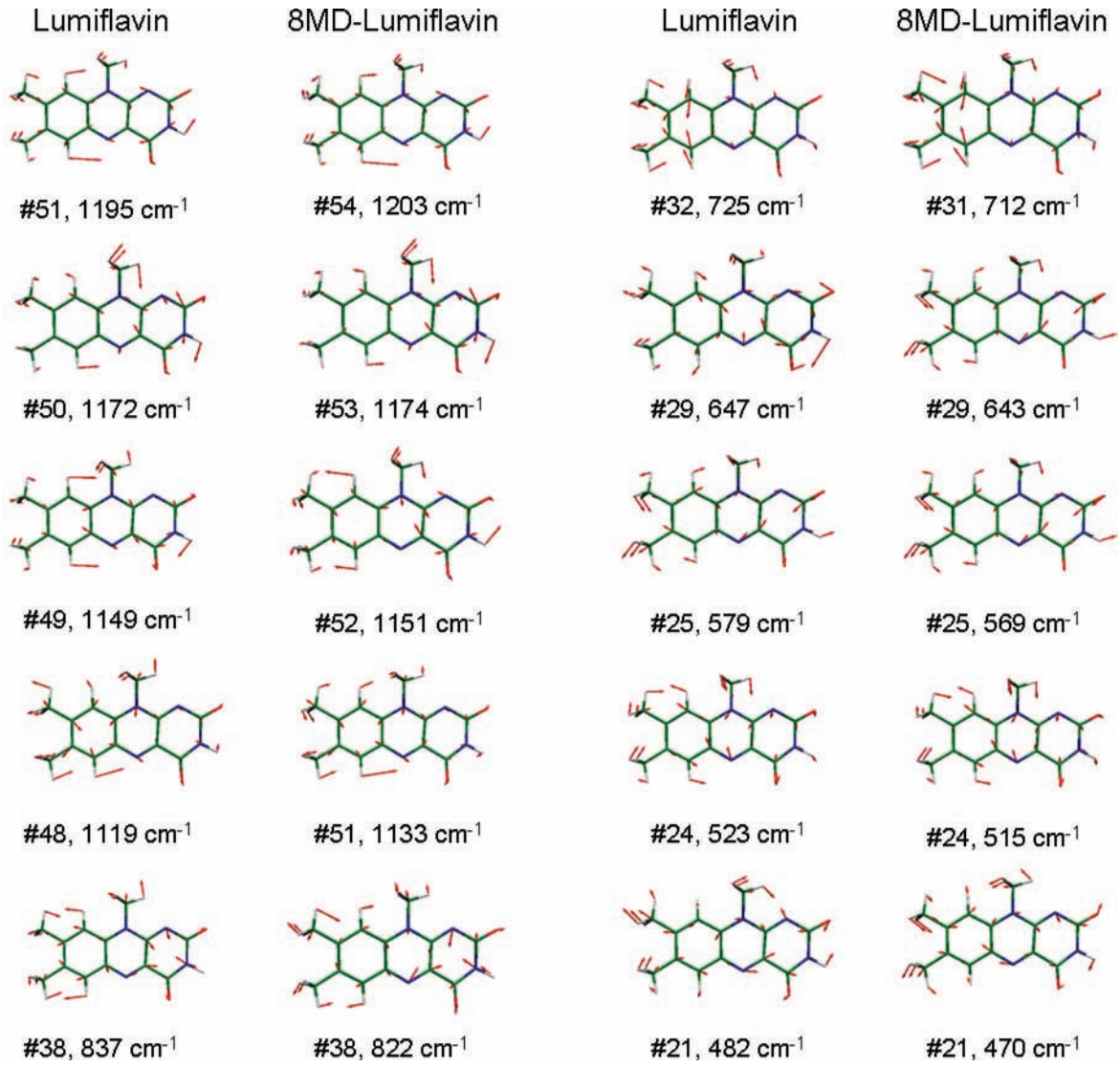

Figure 7. Calculated displacement of LF vibrational normal modes that are the most sensitive to CH_3. The first and second columns and the third and fourth columns show the results for 8-CH_3LF and 8-CD_3LF of corresponding normal modes. The normal modes are numbered according to the output of Gaussian98 (see also Table 1), and the scaled calculated frequencies are listed.

to the 682 cm^{-1} band were in good agreement with our findings.[18–21]

Effect of Partial Deuteration of the 8-Methyl Group on the FMN Vibrational Normal Modes. Several Raman bands show interesting responses to gradual deuteration of the 8-methyl group of FMN. A combined analysis of the experimental data and computational studies provides a consistent and detailed explanation of these observations. The Raman bands at 1228, 1185, 1163, and 1145 cm^{-1} all shift to higher frequencies only upon complete 8-methyl deuteration (Figure 5). The 1228 cm^{-1} band shows a slight shift toward lower frequencies (1217 cm^{-1}) at first, only to abruptly shift to a higher frequency after complete C8−CH_3 deuteration. The relative intensities in the calculated Raman spectra after single, double, and triple C8−CH_3 deuteration explain this isotope behavior in a qualitatively satisfying way. For the 1228, 1184, 1162, and 1145 cm^{-1} bands, we used the calculated normal modes at 1195, 1172, 1149, and 1119 cm^{-1}, respectively, all of which have a C8−CH_3 stretching (νC8−CH_3) contribution. The calculations show that deuterium exchange of up to two hydrogens causes the experimentally observed small frequency downshift due to the increased mass of the methyl group without any significant change in the normal modes. Upon complete deuteration, the νC8−CH_3 contribution to the normal mode becomes a νC8−C one. The uncoupling of the deuteriums from the C8−C oscillator lowers its reduced mass, causing the observed increase in Raman frequencies. The subtle changes in these four normal modes upon full 8-methyl deuteration are visualized in Figure 7.

In the low-frequency region of the Raman spectrum, the 834 and 742 cm^{-1} bands show a gradual disappearance that is correlated to the gradual appearance of the 806 and 729 cm^{-1} bands, respectively. We have identified the normal modes at 837 and 822 cm^{-1} and at 725 and 712 cm^{-1}, which describe the behavior of the 834/806 and 742/729 cm^{-1} couples, respectively (Figure 5). The calculations show that these normal modes have a significant contribution from νC8−CH_3 and a minor one from a C8−C−H_{ip} in-plane bend, δ(C8−C−H_{ip}). Only when the in-plane hydrogen is deuterated do the normal modes change; the contribution of νC8−CH_3 is strongly diminished, while that of δ(C8−C−D_{ip}) becomes more significant. These changes upon H_{ip}/D_{ip} exchange nicely explain the experimentally observed abrupt shift in frequencies and gradual changes in intensities which follow the probability of finding a deuterium in the in-plane position upon gradual deuteration.

In contrast, the 788, 682, and 611 cm^{-1} Raman bands, which we assign to the calculated normal modes at 757, 647, and 579

cm^{-1}, respectively, show a gradual shift in frequency to 786, 680, and 602 cm^{-1}, respectively. In no case does any significant change in the normal mode occur, and the behavior of the observed 788, 682, and 611 cm^{-1} bands is best described by a pure mass effect on the vibrational frequency following gradual deuteration. The subtle changes (or lack thereof) in the normal modes upon complete 8-methyl deuteration in the low-frequency region are visualized in Figure 7.

Our experimental data and computational results show that relatively simple changes in the Raman spectrum upon 8-methyl deuteration of FMN have a more complex underlying behavior. In the high-frequency region, normal modes with a $\nu(C8-CH_3)$ contribution experience a normal mass effect on their frequencies upon partial deuteration. Complete deuteration uncouples the deuteriums from the motion of the methyl carbon, changing the original $\nu C8-CH_3$ contribution into a $\nu C8-C$ one, which causes an abrupt, small frequency upshift of the normal modes. In the low-frequency region, the effect of gradual deuteration is more complex and can depend on whether an in-plane or an out-of-plane hydrogen is substituted with deuterium. Changes in frequency of a normal mode can be due to a change in the contribution of the 8-methyl group to the normal mode, a simple mass effect, or both. Although Figure 5C,D only shows the calculated LF-CHD_2 spectrum, the observed Raman spectrum of 66% deuterated FMN may have equal contributions of FMN with a singly, doubly and triply deuterated $C8CH_3$ group. The good qualitative agreement between the experimental and computational results indicates that the LF-CHD_2 spectrum suffices to show the trends upon partial $C8-CH_3$ deuteration.

Recent methyl-deuteration experiments on protoheme IX also demonstrate this point.[65] Selective deuteration of the 1- and 3-methyl groups revealed strong coupling to the bending vibrations of the nearby vinyl groups, whereas deuteration of the 5- and 8-methyl groups showed their coupling to the bending vibrations of the nearby propionate groups. These and our studies show that the simple deuteration of a methyl group can significantly and unexpectedly affect the normal modes of large molecules such as porphyrins and flavins and that calculations of the normal modes are necessary to fully understand the effects of these seemingly small changes, especially for the normal modes occurring in the low-frequency region.

Effect of Halogen Substitution at the C8 Position. Substitutions at the 8-position other than with isotopes can affect the electronic structure of the isoalloxazine ring and can change it from the common benzenoid form to the quinonoid form.[35,37,38,66] Flavins that are substituted with a halogen retain their benzenoid structure and will be used for comparison to our results. Bands II, IV, V, VI, XI, and XIII show relatively small changes upon 8-methyl deuteration and halogenation, which is most likely due to no or minor contributions of $C8-CH_3$ to their normal modes. Bands I, VII, and X are sensitive to halogen substitution but not to 8-methyl deuteration, which suggests that their normal modes are affected by a change in electron density but not by a change in mass at the 8-position. Band I, whose normal mode is mainly located on ring I, shows a steady decrease in frequency with decreasing electron-donating capability from $-CH_3$ to $-Cl$, $-Br$, and $-I$.[37,66] Bands VII and X do not exhibit such a behavior, because their normal modes are only partially located on ring I. Band XI shifts to higher frequency upon 8-methyl deuteration due to a small change in its normal mode. Its frequency decreases to 1210 cm^{-1} for Cl- and Br-substitution and to 1207 cm^{-1} for I-substitution at the 8-position.[36,66] Given the small differences in frequency change with the large change in mass for these substitutions, the frequency change is probably due to a change in the normal mode of band XI. Finally, Nishina et al. observed several changes in the low-frequency Raman spectrum of RF.[34] The bands at 835 and 739 cm^{-1} shift to 819 and 762 cm^{-1}, respectively, in 7,8-dichloro RF, and the latter was assigned to a ring I breathing-like mode in agreement with our results. Upon 8-methyl deuteration of FMN, both bands show a frequency downshift because of a change in their normal modes. Therefore, we propose that the 7,8-dichloro substitution slightly changes the normal mode of the 835 cm^{-1} band, causing a decrease in its frequency. We expect the same to be true for the normal mode of the 739 cm^{-1} band with an additional change in the electron density of ring I. This explains the frequency increase rather than the frequency decrease that was observed for 8-methyl deuteration.

Analysis of the 5-CH_3−FMN$^\bullet$ Raman Spectrum. The resonance Raman spectrum of 5-CH_3−FMN$^\bullet$ is similar to the one reported before,[10] and the improved signal-to-noise reveals more details, allowing for an easier comparison of the spectra that are obtained for the various isotopes and providing a clear view of the low-frequency region of the spectrum. It also resembles those of other flavin neutral radical semiquinones (FlH$^\bullet$) with a hydrogen atom at the N5 position.[28,29,31,63] The 1592 cm^{-1} band is missing in the Raman spectrum of FlH$^\bullet$, though a shoulder appears at 1593 cm^{-1} upon N−H/D exchange of FlH$^\bullet$ in D_2O. This suggests that the peak at 1605−1617 cm^{-1} is due to coincidental overlap of two normal modes, one of which is sensitive to the mass of the atom or group, i.e., −H, −D, or $-CH_3$, at the N5-position. It has been proposed that this normal mode has a contribution from δN5H,[30–32] which apparently uncouples from the mode upon substitution of the N5−H with D or CH_3. Substitution of $C8-CH_3$ with $-OCH_3$ also affects the main peak at 1617 cm^{-1} of RFH$^\bullet$ in RBP and splits it into 1623 and 1615 cm^{-1} lines, of which the latter shifts to 1604 cm^{-1} in D_2O.[27] This supports the notion of two accidentally overlapping normal modes; one mode is located on ring I and sensitive to changes in the electron-donating ability of the group at the 8-position, and the other mode has a strong contribution from N5−H. The band at 1516 cm^{-1} may have a weak FlH$^\bullet$ counterpart at 1507 cm^{-1}.[67] The more intense 1480 cm^{-1} band does not seem to have an equivalent in FlH$^\bullet$, which suggests that it may be associated with a normal mode that likely involves the $N5-CH_3$. The vibrations between 1050 and 1450 cm^{-1} all seem to have counterparts in FlH$^\bullet$, and small differences in frequencies and intensities may be related to the difference in environment or to small changes in the normal modes due to replacement of the N5 hydrogen with $-CH_3$.

The band at 1179 cm^{-1} was previously proposed to be related to band XI of FMN at 1228 cm^{-1} because of the similarities of the frequency shifts in 8-Cl,5-CH_3−FMN$^\bullet$ and in 8-Cl−FMN.[10] However, in our 8-methyl deuteration experiments, the 1228 cm^{-1} band shifts to 1236 cm^{-1} in FMN, whereas the 1179 cm^{-1} band of 5-CH_3−FMN$^\bullet$ does not change appreciably upon 8-methyl deuteration. Therefore, we rule out that this band is related to the 1228 cm^{-1} band of FMN.

In D_2O, the general trend of changes in the Raman bands of 5-CH_3−FMN$^\bullet$ in the high-frequency region is very similar to that observed for FMN, namely, very small or no frequency shifts above 1300 cm^{-1} and a more complex shifting pattern for the bands between 1100 and 1300 cm^{-1}. This is not too surprising, because for both molecules only N3−H can be exchanged with deuterium in D_2O. In an earlier study, it was thought that the 1283 cm^{-1} band was very sensitive to N3−H/D exchange.[10] However, we measure only a 1 cm^{-1} shift in its

position, and we rule out that the normal mode of this Raman band has any significant contribution from δN3H.

The changes upon N3−H/D and C8−CH_3/D_3 exchange are more significant in the low-frequency region. The 742, 553, and 531 cm^{-1} bands of 5-CH_3FMN$^\bullet$ show isotope shifts very similar to the 742, 539, and 505 cm^{-1} bands of FMN, respectively. This suggests that they may represent very similar normal modes in both molecules, because they also occur at comparable frequencies. We propose that the normal mode of the 742 cm^{-1} band of 5-CH_3−FMN$^\bullet$ is located on ring I with νC−CH_3 contributions and that the one of the 553 cm^{-1} band is located on ring II with $\delta(C_9C_8C_m)$ and $\delta(C_6C_7C_m)$ contributions. The ring I assignment of the 742 cm^{-1} band is in agreement with the shift of the 747 cm^{-1} band in 8-OCH− RFH$^\bullet$ in RBP.[27] Following the assignment of the 505 cm^{-1} band of FMN, we tentatively assign the 531 cm^{-1} band of 5-CH_3−FMN$^\bullet$ to ring I and III deformations with $\delta(C_7C_8C_m)$ and $\delta(C_8C_7C_m)$ contributions. The 891, 877, 787, and 658 cm^{-1} Raman bands are sensitive to both N3−H/D and C8−CH_3/D_3 exchange, and their associated normal modes are expected to have contributions from these two groups, whereas the 607 cm^{-1} band shows sensitivity only to 8-methyl deuteration. Although most observed Raman bands in the low-frequency spectrum of 5-CH_3−FMN$^\bullet$ can be found in previously published low-frequency spectra of FlH$^\bullet$,[17,27] the 891 cm^{-1} does not seem to have any equivalent in the FlH$^\bullet$. This suggests that this band is related to a normal mode with a contribution from N5−CH_3. In H_2O, the 686 cm^{-1} band shifts to a lower frequency upon 8-methyl deuteration, but it is not sensitive to C8−CH_3/D_3 exchange in D_2O. Therefore, we propose that its normal mode has contributions from both N3−H and C8−CH_3, and that N3−H/D exchange changes the normal mode significantly to the extent that it loses its sensitivity to C8−CH_3/D_3 exchange in D_2O.

Conclusions

Resonance Raman spectroscopy and isotopic labeling were used to identify the vibrational normal modes of FMN and of its N5-methyl radical that have a contribution from the 8-methyl group. Although 8-methyl deuteration affects several Raman bands above 1000 cm^{-1} in both molecules, it has a more significant effect on the Raman bands below 1000 cm^{-1}. These data suggest that involvement of the 8-methyl group in protein function is best detected in the low-frequency region of the resonance Raman spectrum. This is especially true for the N5-methyl FMN, where the only significantly sensitive isotope shifts occurred below 1000 cm^{-1}. Partial deuteration experiments on FMN and DFT calculations on partially deuterated lumiflavin have provided deeper insight into the effect of 8-methyl deuteration on the composition of the normal modes. Besides the expected mass effect of the deuteration, there are also mode changes due to decoupling, which are sometimes dependent on whether the exchanged hydrogen is positioned in-plane or out-of-plane. The strong agreement between the experimentally determined and theoretically predicted isotope shifts in this work demonstrates that this combined approach provides a deeper insight into the effect of isotopes on the composition of vibrational normal modes and a better assignment of these modes to the experimentally observed Raman bands. Although we are confident about our assignments, the agreement between the observed and calculated Raman spectra may be further improved by calculating resonance Raman intensities and by the determination of scaling factors for flavin molecules for the use of the scaled quantum mechanics force field approach in future work.

Acknowledgment. This research was supported by NSF Award MCB-0416511 and the ACS Petroleum Research Fund Award AC-42200-AC6. Components of this work were conducted in a Shared Instrumentation Facility at NYU constructed with support from Research Facilities Improvement Grant No. C06 RR-16572 from the NCRR/NIH.

Supporting Information Available: Coordinates of all the optimized geometries of the various isotopes of lumiflavin and the calculated frequencies and Raman intensities. This material is available free of charge via the Internet at http://pubs.acs.org.

References and Notes

(1) Massey, V.; Williams, C. *Flavins and Flavoproteins*; Elsevier: North Holland, 1982.
(2) Muller, F. *Chemistry and Biochemistry of Flavoenzymes, Vol. 1*; CRC Press: Boca Raton, FL, 1991.
(3) Murataliev, M. B.; Feyereisen, R.; Walker, F. A. *Biochim. Biophys. Acta* **2004**, *1698*, 1.
(4) Iyanagi, T. *Biochem. Biophys. Res. Commun.* **2005**, *338*, 520.
(5) Massey, V.; Stankovich, M.; Hemmerich, P. *Biochemistry* **1978**, *17*, 1.
(6) Massey, V.; Palmer, G. *Biochemistry* **1966**, *5*, 3181.
(7) Bretz, N.; Mastalsky, I.; Eisner, M.; Kurreck, H. *Angew. Chem. Int. Ed. Engl.* **1987**, *26*, 4.
(8) Kurreck, H.; Bretz, N. H.; Helle, N.; Henzel, N.; Weilbacher, E. *J. Chem. Soc., Faraday Trans. 1* **1988**, *84* (10), 3293.
(9) Kemal, C.; Chan, T. W.; Bruice, T. C. *Proc. Natl. Acad. Sci. U.S.A.* **1977**, *74*, 405.
(10) Benecky, M. J.; Copeland, R. A.; Spiro, T. G. *Biochim. Biophys. Acta* **1983**, *760*, 163.
(11) Clark, R. J.; Hester, R. E. *Spectroscopy of Biological Systems, Advances in Spectroscopy V1B*; John Wiley & Sons: New York, 1986.
(12) Spiro, T. G. *Biological Applications of Raman Spectroscopy V2: Resonance Raman of Polyenes and Aromatics*; J. Wiley & Sons: New York, 1987.
(13) McFarland, J. T. *Biological Applications of Raman Spectroscopy: Resonance Raman Spectra of Polyenes and Aromatics*; J. Wiley and Sons: New York, 1987.
(14) Kim, M.; Carey, P. R. *J. Am. Chem. Soc.* **1993**, *115*, 7015.
(15) Tegoni, M.; Gervais, M.; Desbois, A. *Biochemistry* **1997**, *36*, 8932–8946.
(16) Kitagawa, T.; Nishina, Y.; Kyogoku, Y.; Yamano, T.; Ohishi, N.; Takai-Suzuki, A.; Yagi, K. *Biochemistry* **1979**, *18*, 1804.
(17) Nishina, Y.; Tojo, H.; Shiga, K. *J. Biochem.* **1988**, *104*, 227.
(18) Bowman, W. D.; Spiro, T. G. *Biochemistry* **1981**, *20*, 3313.
(19) Copeland, R. A.; Spiro, T. G. *J. Phys. Chem.* **1986**, *90*, 6648.
(20) Abe, M.; Kyogoku, Y. *Spectrochim. Acta* **1987**, *43A*, 1027.
(21) Lively, C. R.; McFarland, J. T. *J. Phys. Chem.* **1990**, *94*, 3980.
(22) Zheng, Y.; Dong, J.; Plafey, B. A.; Carey, P. R. *Biochemistry* **1999**, *38*, 16727.
(23) Swartz, T. E.; Wenzel, P. J.; Corchnoy, S. B.; Briggs, W. R.; Bogomolni, R. A. *Biochemistry* **2002**, *41*, 7183.
(24) Wille, G.; Ritter, M.; Friedemann, R.; Mantele, W.; Hubner, G. *Biochemistry* **2003**, *42*, 14814.
(25) Unno, M.; Sano, R.; Masuda, S.; Ono, T.; Yamauchi, S. *J. Phys. Chem. B* **2005**, *109*, 12620.
(26) Nishina, Y.; Shiga, K.; Miura, R.; Tojo, H.; Ohta, M.; Miyake, Y.; Yamano, T.; Watari, H *J. Biochem* **1983**, *94*, 1979.
(27) Nishina, Y.; Shiga, K.; Horiike, K.; Tojo, H.; Kasai, S.; Matsui, K.; Watari, H.; Yamano, T. *J. Biochem.* **1980**, *88*, 411.
(28) Sugiyama, T.; Nisimoto, Y.; Mason, H. S.; Loehr, T. M. *Biochemistry* **1985**, *24*, 3012.
(29) Su, Y.; Tripathi, G. N. R. *J. Am. Chem. Soc.* **1994**, *116*, 4405.
(30) Murgida, D. H.; Schleicher, E.; Bacher, A.; Richter, G.; Hildebrandt, P. *J. Raman. Spectrosc.* **2001**, *32*, 551.
(31) Schelvis, J. P. M.; Ramsey, M.; Sokolova, O.; Tavares, C.; Cecala, C.; Connell, K.; Wagner, S.; Gindt, Y. M. *J. Phys. Chem. B* **2003**, *107*, 12352.
(32) Li, J.; Uchida, T.; Ohta, T.; Todo, T.; Kitagawa, T. *J. Phys. Chem.* **2006**, *110*, 16724.
(33) Romich, W.; Eisenreich, W.; Richter, G.; Bacher, A. *J. Org. Chem.* **2002**, *67*, 8890.
(34) Nishina, Y.; Kitagawa, T.; Shiga, K.; Horiike, K.; Matsumura, Y.; Watari, H.; Yamano, T. *J. Biochem.* **1978**, *84*, 925.
(35) Dutta, P. K.; Spencer, R.; Walsh, C.; Spiro, T. G. *Biochim. Biophys. Acta* **1980**, *623*, 77.
(36) Schopfer, L. M.; Morris, M. D. *Biochemistry* **1980**, *19*, 4932.

(37) Schopfer, L. M.; Haushalter, J. P.; Smith, M.; Milad, M.; Morris, M. D. *Biochemistry* **1981**, *20*, 6734.
(38) Schmidt, J.; Lee, M.; McFarland, J. T. *Arch. Biochem. Biophys.* **1982**, *215*, 22.
(39) Powell, J. F. *Biochem. Soc. Trans.* **1991**, *19*, 199.
(40) Binda, C.; Mattevi, A.; Edmondson, D. E. *J. Biol. Chem.* **2002**, *277*, 23973.
(41) Wang, M.; Roberts, D. L.; Paschke, R.; Shea, T. M.; Masters, B. S.; Kim, J. J. *Proc. Natl. Acad. Sci.* **1997**, *94*, 8411.
(42) Mees, A.; Klar, T.; Gnau, P.; Hennecke, U.; Eker, A. P. M.; Carell, T.; Essen, L. *Science* **2004**, *306*, 1789.
(43) Gindt, Y. M.; Schelvis, J. P. M.; Thoren, K. L.; Huang, T. H. *J. Am. Chem. Soc.* **2005**, *127*, 10472.
(44) Li, J.; Uchida, T.; Todo, T.; Kitagawa, T. *J. Biol. Chem.* **2006**, *281*, 25551.
(45) Bullock, F. J.; Jardetzky, O *J. Org. Chem.* **1965**, *30*, 2056.
(46) Entsch, B.; Sim, R. G. *Anal. Biochem.* **1983**, *133*, 401.
(47) Becke, A. D. *J. Chem. Phys.* **1993**, *98*, 5648.
(48) Ditchfield, R.; Hehre, W. J.; Pople, J. A. *J. Chem. Phys.* **1972**, *56*, 2257.
(49) Deppmeier, B. J.; Driessen, A. J.; Hehre, T. S.; Hehre, W. J.; Johnson, J. A.; Klunzinger, P. E.; Leonard, J. M.; Pham, I. N.; Pietro, W. J.; Yu, J.; Kong, J.; White, C. A.; Krylov, A. I.; Sherrill, C. D.; Adamson, R. D.; Furlani, T. R.; Lee, M. S.; Lee, A. M.; Gwaltney, S. R.; Adams, T. R.; Ochsenfeld, C.; Gilbert, A. T. B.; Kedziora, G. S.; Rassolov, V. A.; Maurice, D. R.; Nair, N.; Shao, Y.; Besley, N. A.; Maslen, P. E.; Dombroski, J. P.; Dachsel, H.; Zhang, W. M.; Korambath, P. P.; Baker, J.; Byrd, E. F. C.; Van Voorhis, T.; Oumi, M.; Hirata, S.; Hsu, C. P.; Ishikawa, N.; Florian, J.; Warshel, A.; Johnson, B. G.; Gill, P. M. W.; Head-Gordon, M.; Pople, J. A. *Spartan '02*; Wavefunction Inc.: Irvine, CA, 1992.
(50) Frisch, M. J.; Trucks, G. W.; Schlegel, H. B.; Scuseria, G. E.; Robb, M. A.; Cheeseman, J. R.; Zakrzewski, V. G.; Montgomery, J. A., Jr.; Stratmann, R. E.; Burant, J. C.; Dapprich, S.; Millam, J. M.; Daniels, A. D.; Kudin, K. N.; Strain, M. C.; Farkas, O.; Tomasi, J.; Barone, V.; Cossi, M.; Cammi, R.; Mennucci, B.; Pomelli, C.; Adamo, C.; Clifford, S.; Ochterski, J.; Petersson, G. A.; Ayala, P. Y.; Cui, Q.; Morokuma, K.; Malick, D. K.; Rabuck, A. D.; Raghavachari, K.; Foresman, J. B.; Cioslowski, J.; Ortiz, J. V.; Baboul, A. G.; Stefanov, B. B.; Liu, G.; Liashenko, A.; Piskorz, P.; Komaromi, I.; Gomperts, R.; Martin, R. L.; Fox, D. J.; Keith, T.; Al-Laham, M. A.; Peng, C. Y.; Nanayakkara, A.; Gonzalez; Challacombe, C. M.; Gill, P. M. W.; Johnson, B.; Chen, W.; Wong, M. W.; Andres, J. L.; Gonzalez, C.; Head-Gordon, M.; Replogle, E. S.; Pople, J. A. *Gaussian 98*, revision A.7; Gaussian, Inc.: Pittsburgh, PA, 1998.
(51) Pulay, P.; Fogarasi, G.; Pongor, G.; Boggs, J. E.; Vargha, A. *J. Am. Chem. Soc.* **1983**, *105*, 7037.
(52) Baker, J.; Jarzecki, A. A.; Pulay, P. *J. Phys. Chem. A* **1998**, *102*, 1412.
(53) Kozlowski, P. M.; Jarzecki, A. A.; Pulay, P. *J. Phys. Chem.* **1996**, *100*, 7007.
(54) Scott, A. P.; Radom, L. *J. Phys. Chem.* **1996**, *100*, 16502.
(55) Brand, H. V.; Rabie, R. L.; Funk, D. J.; Diaz-Acosta, I.; Pulay, P.; Lippert, T. K. *J. Phys. Chem. B* **2002**, *106*, 10594.
(56) Keresztury, G.; István, K.; Sundius, T. *J. Phys. Chem. A* **2005**, *109*, 7938.
(57) Mroginski, M. A.; Murgida, D. H.; Hildebrandt, P. *J. Phys. Chem. A* **2006**, *110*, 10564.
(58) Laaksonen, L. *gOpenMol Version 2.3*; Center for Scientific Computing: Espoo, Finland, 2003.
(59) Benecky, M.; Li, T. Y.; Schmidt, J.; Frerman, F.; Watters, K. L.; McFarland, J. *Biochemistry* **1979**, *18*, 3471.
(60) Schmidt, J.; Coudron, P.; Thompson, A. W.; Watters, K.; McFarland, J. T. *Biochemistry* **1983**, *22*, 76.
(61) Nishina, Y.; Sato, K.; Miura, R.; Matsui, K.; Shiga, K. *J. Biochem.* **1998**, *124*, 200.
(62) Hazekawa, I.; Nishina, Y.; Sato, K.; Shichiri, M.; Miura, R.; Shiga, K. *J. Biochem.* **1997**, *121*, 1147.
(63) Kitagawa, T.; Sakamoto, H.; Sugiyama, T.; Yamano, T. *J. Biol. Chem.* **1982**, *257*, 12075.
(64) Dutta, P. K.; Nestor, J.; Spiro, T. G. *Biochem. Biophys. Res. Commun.* **1978**, *83*, 209.
(65) Mak, P. J.; Podstawka, E.; Kincaid, J. R.; Proneiwicz, L. M. *Biopolymers* **2004**, *75*, 217–228.
(66) Nishina, Y.; Shiga, K.; Horiike, K.; Tojo, H.; Kasai, S.; Yanase, K.; Matsui, K.; Watari, H.; Yamano, T. *J. Biochem.* **1980**, *88*, 403.
(67) Sokolova, O.; Cecala, C.; Gopal, A.; Cortazar, F.; McDowell-Buchanan, C.; Sancar, A.; Gindt, Y. M.; Schelvis, J. P. M. *Biochemistry* **2007**, *46*, 3673.

JP711832G